Marsdenia tenacissima extract alters crucial metabolites in cancer, determined by ¹H NMR based metabolomics approach

Debmalya Roy[2], Cheng Chen[3], Jun-song Wang[3*], Shengtao Yuan[1*], Li Sun[2*]

[1]Jiangsu Key Laboratory of Drug Screening, China Pharmaceutical University, Nanjing, China, [2]Jiangsu Center for Pharmacodynamics Research and Evaluation, China Pharmaceutical University, Nanjing, China, [3]Center for Molecular Metabolism, School of Environmental and Biological Engineering, Nanjing University of Science and Technology, 200 Xiao Ling Wei Street, Nanjing, PR China

Altered metabolites level in the biosystems, is the potential cause of cancer, the primary reason of alteration of metabolism is change in nutrient consumption and waste excretion, as a result genetic mutation leads to cancer initiation and progression. Aberration of specific metabolites such as fumarate, succinate, 2-hydroxyglutarate may alter cell signaling. We collected liver and kidney samples and prepared for ¹H NMR analysis, then executed NMR spectroscopy. We used a set of domestic R scripts to perform an unsupervised principal component analysis (PCA) and a supervised orthogonal signal correction partial least-squares discriminant analysis (OSC-PLS-DA). It signifies class discrimination for getting a clear separation, whereas PCA scores plot signifies the model group kept further away from the control group than drug group on the horizontal axis. In another PCA scores plots, most parts of the control group was overlapping with the drug group but was distant from the model group. Marsdenia tenacissima extract (MTE) (Chines name: Xiao-Ai-Ping, XAP) modulates level of crucial metabolites such as fumarate, lactate, succinate, determined by ¹H NMR spectroscopy and their altered level contributes major role in cancer.

Keywords: Marsdenia tenacissima extract (MTE). MDA-MB-231. ¹H NMR. Metabolomics.

INTRODUCTION

MTE is an anti-cancer, traditional Chinese herbal medicine. It has been widely used in various diseases and also in cancer, for many decades. But previously, no metabolomics study is carried out on MTE. In this research study, we explored the anticancer action of MTE in order to metabolomics approach, that how the level of some metabolites directly or indirectly involved with progression and suppression of cancer, modulated by MTE.

Metabolomics is a kind of newly emerging subject in recent decades which focuses on the changes of all the metabolites produced by external stimulus in the biosystem. This process is used to track the biomarkers according to the changes of the metabolic fingerprint and illuminate the overall effect (Roy *et al.,* 2017), now metabolomics methods have been widely employed in recent years (Griffin, 2004; Lou *et al.,* 2015). We unveiled in this research study, that some crucial metabolites play a major role in cancer. Mainly, the overexpression of succinate (Selak *et al.,* 2005) and lactate (Hirschhaeuser, Sattler, Mueller-Klieser, 2011) links with cancer formation. The aim of this research was to investigate the curative effect of MTE on MDA-MB-231 in nude mice at the dosage of 2.5g/kg, using an NMR based metabolomics approach complemented with the histological inspection.

MATERIAL AND METHOD

Sample collection and preparation for ¹H NMR analysis

After three weeks of the treatment, all mice fasted overnight. The next day after the final administration of MTE and after anesthetization by chloral hydrate (350 mg kg⁻¹, i.p.) all of them were sacrificed. Their

*Correspondence: Jun-Song Wang. Center for Molecular Metabolism, School of Environmental and Biological Engineering, Nanjing University of Science and Technology, 200 Xiao Ling Wei Street, Nanjing 210094, PR China. E-mail: wang.junsong@gmail.com.

Braz. J. Pharm. Sci. 2018;54(2):e17604

Page 1 / 8

livers and kidneys were harvested and frozen in the liquid nitrogen and stored at -80 ℃ immediately. Before ¹H NMR analysis, frozen mice liver and kidney tissues were weighted (500 mg) and homogenized in 50% acetonitrile/H_2O (3 mL) and centrifuged at 12000 rpm for 10 min at 4 °C. We collected the supernatant. And then, the supernatant was lyophilized and reconstituted in 550 µL D_2O in phosphate-buffered solution (0.2 M Na_2HPO_4 –NaH_2PO_4, pH 7.4). We used TSP (0.05 wt%) as an internal standard for D_2O. The supernatant was transferred into a 5 mm NMR tube for ¹H NMR analysis after the solution was vortexed and centrifuged at 12000 rpm for 10 min to remove any debris. D_2O was used for field frequency locking and TSP was used as a chemical shift reference (¹H, 0.00 ppm).

¹H NMR spectroscopy

All the ¹H NMR spectra of liver and kidney samples were acquired at 298 K on a Bruker Avance 500 MHz flow-injection spectrometer (Bruker GmbH, Karlsruhe, Germany) with a Bruker 5 mm probe, using a modified transverse relaxationedited Call-Purcell-Meiboom-Gill (CPMG) sequence (90(τ–180-τ) n-acquisition) with a total spin-echo delay (2nτ) of 10 ms to suppress the signals of proteins, with 128 transients collected into 32 768 (32 K) data points, a spectral width of 10 000 Hz, an acquisition time of 3.27 s. The spectra were Fourier transformed after multiplying the FIDs by an exponential weighting function corresponding to a line-broadening of 0.5 Hz.

Data pre-processing and peak assignments

The ¹H NMR spectra were phased and baseline-corrected manually using Bruker Topspin 3.0 software (Bruker GmbH, Karlsruhe, Germany). The spectra were converted to ASCII-format files by using MestReNova (Version 8.0.1, Mestrelab Research SL) and then imported into "R" (http://cran.r-project.org/) for multivariate data analysis using internally developed R scripts. The spectra were split into 0.015 ppm average integrated spectral regions (buckets) between 0.2 and 10 ppm. Then, the data were probability quotient-normalized to account for variation in sample dilutions. We assigned the metabolites in the NMR spectra according to the previous literature and queried performed in open access databases, such as the Madison metabolomics consortium database (http://mmcd.nmrfam.wisc.edu/) and the human metabolome database (http://www.hmdb.ca/). We also used Chenomx NMR suite 7.7 software and the statistical total correlation spectroscopy (STOCSY) technique to assign the metabolites.

Data analysis

We used a set of domestic R scripts to perform an unsupervised PCA and a supervised OSC-PLS-DA. PCA was performed to show a general overview of the metabolic pattern through using the NMR data and then, OSC-PLS-DA was performed to show differences in metabolic alterations across the liver and kidney tissues. Each OSC-PLS-DA model was confirmed by repeated two-fold cross-validation, as follows: the validity of the model against overfitting was assessed using the parameter R^2Y, and the predictive ability was described by Q^2.

Color-coded loading and S-plots were constructed to illustrate the variables that contributed to the grouping. The fold changes and the associated p-values adjusted by BH (Benjamini–Hochberg) methods of different metabolites in liver and kidney samples were calculated and listed in Table I (for liver samples) and Table II (for kidney samples).

RESULTS AND DISCUSSION

Multivariate analysis of ¹H NMR spectra

We used the supervised OSC-PLS-DA to remove variations that were unrelated to class discrimination for getting a clear separation. In the PCA scores plots of the liver (Figure 1A), the model group kept further away from the control group than drug group on the horizontal axis. In another PCA scores plots (Figure 1B for kidney), most parts of the control group were overlapping with the drug group but were distant from the model group.

The loading plot (Figure 1B, C, E, F) was constructed by a covariance-based pseudo-spectrum and it was used to show color-coded according to the absolute values of the correlation coefficients (r^2). The weight of a variable in the discrimination model was determined by calculating the square of its r^2 and ranged from zero (blue areas) to high values (red areas). Changes in metabolites were directly visualized as fold-changes in these plots (Figure 2). They are color-coded according to the p-values of differences among the groups.
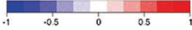
In this study, we also analyzed the antitumor activity of MTE with ¹H NMR-based metabolomics approach. OPLS-DA analysis of NMR data from livers and kidneys revealed that MTE induced severe metabolic perturbations (Figure 3). Both of the livers and kidneys' model groups were found with the significant higher level of succinate. It can be catalyzed into fumarate by succinate dehydrogenase (SDH). SDH is also a tumor suppressor. The succinate accumulated in the mitochondria due to

Page 2 / 8

Braz. J. Pharm. Sci. 2018;54(2):e17604

TABLE I - Identified metabolites in the livers from different groups with $\log_2(FC)$ and p-values [a] Multiplicity: singlet (s), doublet (d), triplet (t), quartets (q), multiplets (m). [b] Color coded according to the log2(FC), red represents increased and blue represents decreased concentrations in glyphosate exposed groups. Color bar ▇▇▇ [c] p-values corrected by BH (Benjamini Hochberg) methods were calculated based on a parametric Student's t-test or a nonparametric Mann–Whitney test (dependent on the conformity to normal distribution). *p < 0.05, **p < 0.01, ***p < 0.001

Metabolites	Chemical shift (ppm)[a]	C vs. M		C vs. H	
		$\log_2(FC)$[b]	P[c]	$\log_2(FC)$	P
Valine	1.05(d)	-0.15		0.09	
Isoleucine	1.00(t)	-0.16		0.14	
Leucine	0.95(t)	-0.01		0.19	*
3-Hydroxybutyrate	1.21(d)	-0.02		-0.52	*
Lactate	1.33(d),4.12(t)	0.02		-0.39	**
Alanine	1.49(d)	0.11		0.06	
Acetate	1.93(d)	0.14		0.28	*
Glutamate	2.08(m),2.35(m)	0.19	*	0.25	***
Succinate	2.41(s)	1.19	**	0.45	
Carnitine	2.47(m)	-0.45	*	-0.08	
Methionine	2.66(q)	0.14		0.29	**
Creatine	3.04(s)	0.23		0.37	**
Ethanolamine	3.14(t)	0.39		0.18	
Choline	3.21(s)	-0.05		0.01	
Taurine	3.28(t),3.42(m)	-0.04		0.04	
myo-Inositol	3.62(m),4.07(q)	0.22	**	0.17	**
Betaine	3.92(s)	-0.24		-0.20	
Glucose	3.80(m),5.24(d)	-0.18	*	-0.18	**
Uracil	5.81(d),7.55(d)	0.07		-0.23	*
Inosine	6.11(d),8.36(s)	0.24		0.29	*
Fumarate	6.53(s)	0.14		-0.02	
Tyrosine	6.91(d),7.20(d)	-0.05		-0.10	
Niacinamide	7.60(q),8.72(q),8.95(d)	0.09		-0.01	
Theophylline	8.01(s)	-0.11		0.02	
ATP	8.51(s)	0.36		-0.08	
AMP	8.59(s)	0.07		-0.01	

SDH inhibition is transported to the cytosol. Elevated cytosolic succinate inhibits HIF-prolyl hydroxylase (PHD) and thereby Hypoxia-inducible factor-α (HIF-α) hydroxylation. HIF-α makes up HIF combined with HIF-β. In many tumors, oxygen availability becomes limited (hypoxia) very quickly during cancer development. Intermittent hypoxia may paradoxically be the only reason for increased tumor glycolysis (Zu, Guppy, 2004). The major regulator of the response to hypoxia is the HIF transcription factor, forcefully, emphasizing the importance of HIF in tumor development or sustention. In addition, it was demonstrated that HIF activation resulting from von Hippel-Lindau (VHL) mutations promotes metastasis by inducing the expression of met and CXR4 (Selak *et al.*, 2005). The VHL gene product (pVHL) is part of an E3 ubiquitin ligase complex that binds to the oxygen-dependent degradation (ODD) domain of HIF-α in an oxygen-dependent manner and targets it for degradation (Pugh, Ratcliffe, 2003; Semenza, 2002). Consequently, pVHL binding to HIF-α is decreased, and elevated HIF activity induces expression of genes that facilitate angiogenesis, metastasis, and metabolism, leading to

Braz. J. Pharm. Sci. 2018;54(2):e17604

Page 3 / 8

TABLE II - Identified metabolites in the kidney from different groups with $\log_2(FC)$ and p-values [a] Multiplicity: singlet (s), doublet (d), triplet (t), quartets (q), multiplets (m). [b] Color coded according to the log2(FC), red represents increased and blue represents decreased concentrations in glyphosate exposed groups. Color bar [image] [c] p-values corrected by BH (Benjamini Hochberg) methods were calculated based on a parametric Student's t-test or a nonparametric Mann–Whitney test (dependent on the conformity to normal distribution). *p < 0.05, **p < 0.01, ***p < 0.001

Metabolites	Chemical shift (ppm)[a]	C VS. M		C vs. H	
		$\log_2(FC)$[b]	P[c]	$\log_2(FC)$	P
Valine	1.00(d), 1.05(d)	-0.33		0.21	
Isoleucine	0.94(d), 1.02(d)	-0.20		0.09	
Leucine	0.97(t), 1.68(m)	-0.28		0.10	
3-Hydroxybutyrate	1.20(d)	-0.29		-0.13	
Lactate	1.34(d), 4.12(q)	0.00		-0.02	
Alanine	1.49(d)	0.54	*	0.40	
Acetate	1.93(s)	0.11		0.34	
Succinate	2.41(s)	1.31	**	0.84	*
Lysine	1.73(q), 1.90(q), 3.03(s)	-0.36		0.04	
Creatine	3.04(d)	-0.05		-0.12	
Glutamine	2.13(t), 2.46(q)	0.17		0.28	
Glucose	3.25(d), 3.50(m), 3.80(m), 4.66(d), 5.24(d)	-0.06		-0.02	
Taurine	3.27(t)	-0.20		0.01	
Glutamate	2.34(m), 2.05(t)	0.99	**	0.74	***
Glutathione	2.18(t), 2.56(m), 2.95(m)	0.51	*	0.73	*
Glycine	2.57(s)	-0.05		0.33	
Lactose	4.46(s)	-1.5	**	-0.22	
3-Hydromuconate	5.63(m)	0.58		0.33	
Histamine	3.00(t), 7.12(s), 7.96(s)	0.15		0.19	
sn-Glycero-3-phosphocholine	3.23(s)	0.29		0.43	
Niacinamide	7.60(q), 8.72(d), 8.94(d)	-0.37	*	-0.34	*
Inosine	4.44(d), 6.11(d), 8.24(s), 8.36(s)	-0.82	**	-0.30	*
Maltose	3.64(m), 3.31(s)	-0.90	**	-0.38	
Fumarate	6.53(s)	0.48		1.05	*
Tyrosine	6.90(d), 7.19(d)	-0.37		-0.29	
Phenylalanine	7.38(m)	-0.19		-0.12	
Formate	8.46(s)	-0.05		0.20	
Xanthine	7.92(s)	0.39		0.16	
Uridine	5.91(q), 7.88(s), 7.90(s)	1.12	**	-0.64	
ATP	6.14(d), 8.27(s), 8.51(s)	-0.22		-0.03	
AMP	8.59(s)	0.06		0.15	
3-Hydroxyphenylacetate	6.81(s)	-0.23		-0.45	
Uracil	5.81(d), 7.55(d)	-0.48		-0.50	

more aggressive tumors (Selak *et al.,* 2005). To sum up, succinate may function as an intracellular messenger between mitochondria and the cytosol and has a profound effect on cytosolic enzymes (PHD) and consequently on nuclear events (gene expression by HIF) (Figure 4).

Significant alteration level of metabolites with their related expression and relevant action are summarized in the Table III. All the above indicates that the float of
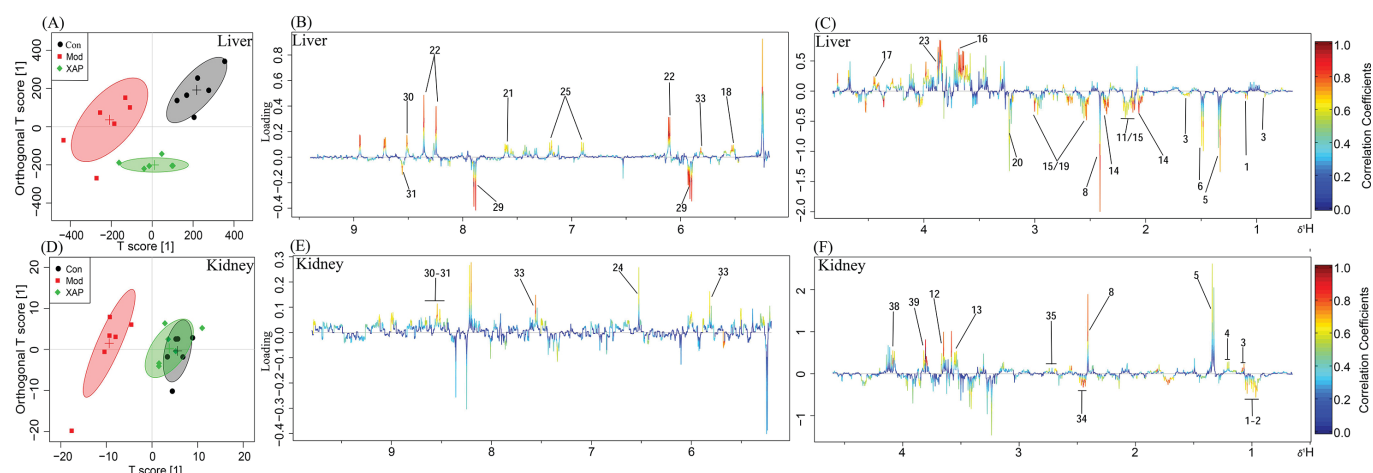
Page 4 / 8

Braz. J. Pharm. Sci. 2018;54(2):e17604

FIGURE 1 - OPLS-DA analysis of liver and kidney extract ^{1}H NMR data of control, model, and MTE groups. Score plots (A for liver, D for kidney) and the corresponding loading plots of OPLS-DA (B and C for liver, E, and F for kidney) color-coded with the absolute value of correlation coefficients. The color bar corresponds to the weight of the corresponding variable in the discrimination of statistically significant (red) or non-significant (blue).Positive and negative peaks indicate a relatively decreased and increased metabolite level.
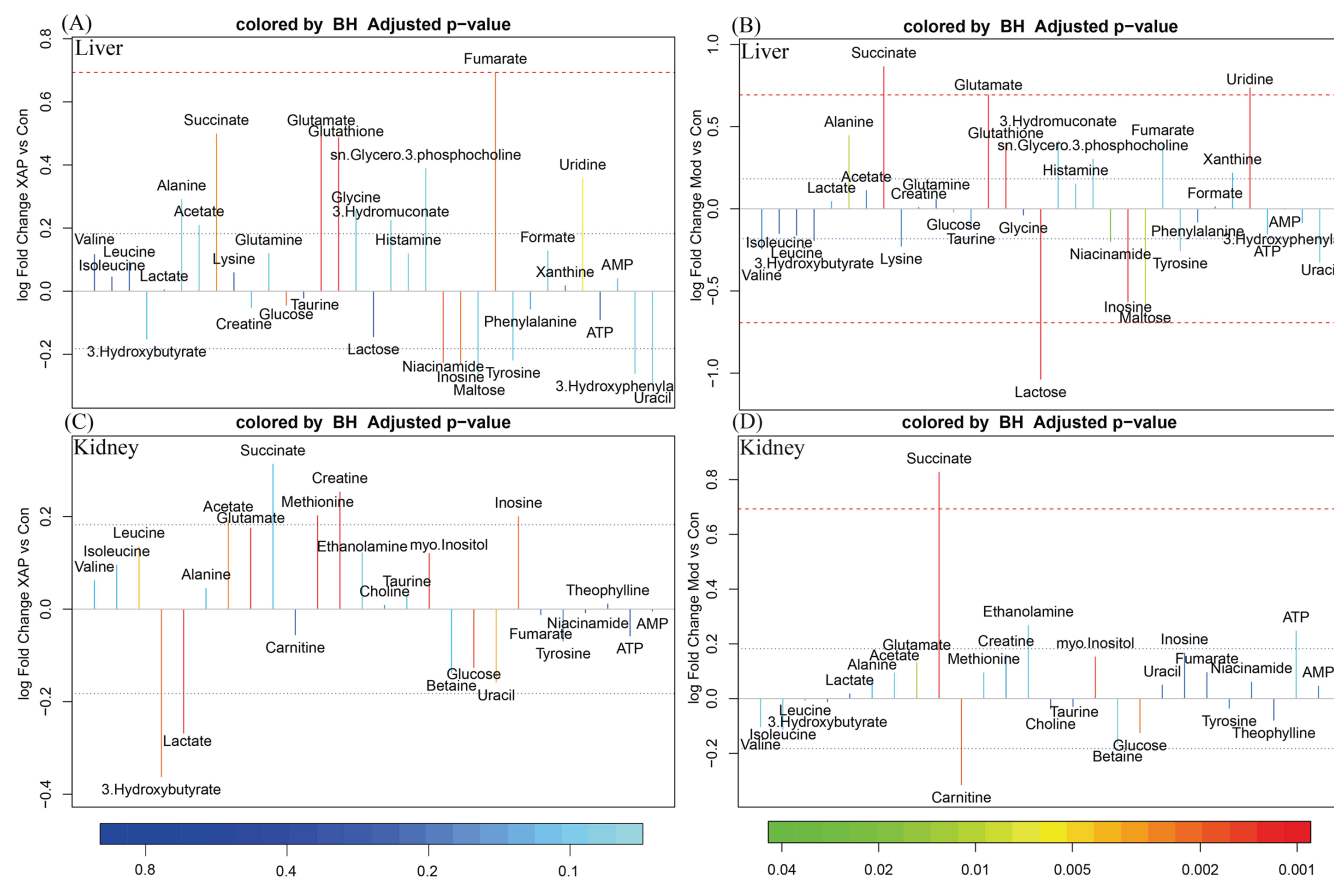
FIGURE 2 - Typical 500 MHz ^{1}H NMR spectra of liver tissue and kidney extracts obtained from Con. (black lines), MTE (XAP) (green lines) and Mod groups (red lines). The metabolites are labeled as follows: 1. Valine, 2. Isoleucine, 3. Leucine, 4. 3-Hydroxybutyrate, 5. Lactate, 6. Alanine, 7. Acetate, 8. Succinate, 9. Lysine, 10. Creatine, 11. Glutamine, 12. Glucose, 13. Taurine, 14. Glutamate, 15. Glutathione, 16. Glycine, 17. Lactose, 18. 3-Hydromuconate, 19. Histamine, 20. sn-Glycero-3-phosphocholine, 21. Niacinamide, 22. Inosine, 23. Maltose, 24. Fumarate, 25. Tyrosine, 26. Phenylalanine, 27. Formate, 28. Xanthine, 29. Uridine, 30. ATP, 31. AMP, 32. 3-Hydroxyphenylacetate, 33. Uracil, 34. Carnitine, 35. Methionine, 36. Ethanolamine, 37. Choline, 38. myo-Inosito, 39. Betaine, and 40. Theophylline.

Braz. J. Pharm. Sci. 2018;54(2):e17604

Page 5 / 8

TABLE III - Different level of metabolites: In liver the level of the metabolites, alanine, succinate, glutamate, lactose and fumarate were aberrated significantly. Alanine (Leij-Halfwerk *et al.,* 2000; Tessem *et al.,* 2008), succinate (Yang, Pollard, 2013), glutamate (Fazzari *et al.,* 2015; Willard, Koochekpour, 2013) are related to the cancer progression. Conversely, lactose (Goodman *et al.,* 2002) and fumarate play a pivotal role in the inhibition of cancer progression. However, in kidney, the level of succinate and lactate (Bonuccelli *et al.,* 2010)were notably reduced, besides this the level of 3-Hydroxybutyrate (Bonuccelli *et al.,*2010) was augmented remarkably, which takes part a major role in tumor progression

| Metabolites	Expression	Role in Cancer	Action	Reference
Alanine	Down	Progression	Elevated level of alanine is the cause of gluconeogenesis leads to lung cancer with weight loss, alanine is the major source of respiratory energy in cancer.	51, 52
Succinate	Down	Progression	Elevated cytosolic succinate inhibits HIFprolyl hydroxylase (PHD) and thereby Hypoxia-inducible factor- α (HIF-α) hydroxylation.	53
Lactate	Down	Progression	Initiation of angiogenesis	57
3-Hydroxybutyrate	Down	Progression	Tumor progression	57
Glutamate	Down	Progression	Induces migration, invasion and inhibition of apoptosis.	54, 55
Lactose	Up	Inhibition	Reduce risk of ovarian cancer.	56
Fumarate	Up	Inhibition	Depletion of the level of fumarate links to accumulation of succinate, leads to activation of HIF-1α.	…..
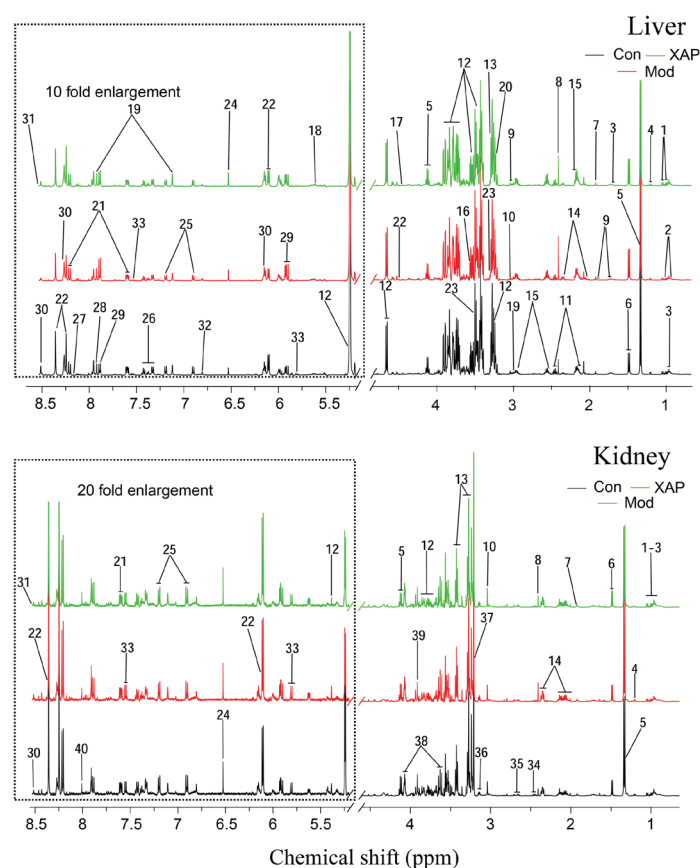
FIGURE 3 - Fold change plots color-coded with p-values adjusted by Benjamini Hochberg method indicating the significance of altered metabolites in the liver of (A), XAP vs. control (B), model vs. control (C), and lung of XAP vs. control (D), model vs. control. The blue and red dashed lines represented variations of 20% and 100%, respectively.
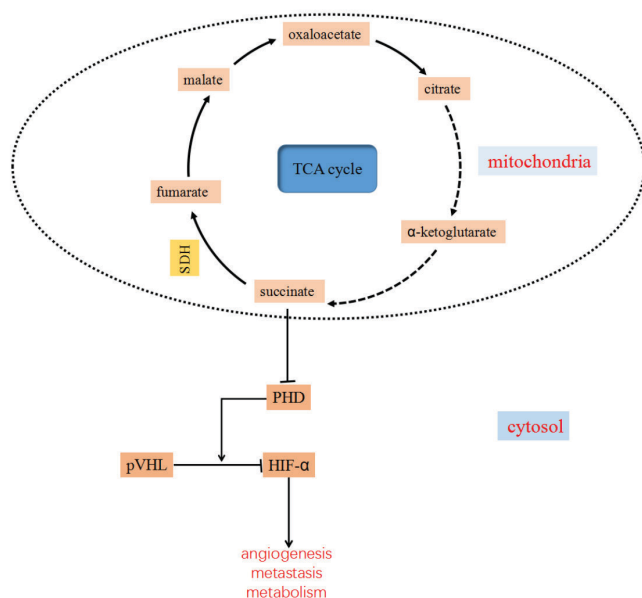
FIGURE 4 - A schematic model that summarizes the role of succinate in the mitochondrion-to-cytosol signaling pathway. Succinate accumulated in the mitochondria due to SDH inhibition is transported to the cytosol. Elevated cytosolic succinate inhibits PHD and thereby HIF-α hydroxylation. Consequently, pVHL binding to HIF-α is decreased, and elevated HIF activity induces expression of genes that facilitate angiogenesis, metastasis, and metabolism, leading to more aggressive tumors (Table I).

succinate can reflect the growth of cancer cells in vivo. After a consecutive 3 weeks oral MTE administration, the level of succinate was significantly lowered and back to normal. In another way, MTE was proved to exhibit antitumor action in vivo.

Here we used xenograft mice model for this study because all mammalian cells have similar biological pathways to regulate growth, differentiation, replication, and death. It has been also observed that Mice and Human have similar metabolic homogeneity and physiology disease pathogenesis. Additionally, mice acquire mutations by the equivalent spectrum of tumor suppressor genes and proto-oncogenes as Human (Balmain, Harris, 2000) (Demetrius, 2005). So, this research outcome also will be effective on Human as well.

CONCLUSION

It has been revealed through ^{1}H NMR-based metabolomics approach that MTE modulates the alteration of crucial metabolites, mainly succinate and lactate, which contribute major role in cancer formation.

REFERENCES

Balmain A, Harris CC. Carcinogenesis in mouse and human cells: parallels and paradoxes. Carcinogenesis. 2000;21(3):371-377.

Bonuccelli G, Tsirigos A, Whitaker-Menezes D, Pavlides S, Pestell RG, Chiavarina B, et al. Ketones and lactate "fuel" tumor growth and metastasis: Evidence that epithelial cancer cells use oxidative mitochondrial metabolism. Cell Cycle. 2010;9(17):3506-3514.

Demetrius L. Of mice and men. EMBO Rep. 2005;6(Suppl 1):S39-S44.

Fazzari J, Lin H, Murphy C, Ungard R, Singh G. Inhibitors of glutamate release from breast cancer cells; new targets for cancer-induced bone-pain. Sci Rep. 2015;5:8380.

Goodman MT, Wu AH, Tung K-H, McDuffie K, Kolonel LN, Nomura AM, et al. Association of dairy products, lactose, and calcium with the risk of ovarian cancer. Am J Epidemiol. 2002;156(2):148-157.

Griffin JL. The potential of metabonomics in drug safety and toxicology. Drug Discov Today Technol. 2004;1(3):285-293.

Hirschhaeuser F, Sattler UGA, Mueller-Klieser W. Lactate: a metabolic key player in cancer. Cancer Res. 2011;71(22):6921-6925.

Leij-Halfwerk S, Dagnelie PC, van den Berg JWO, Wattimena JDL, Hordijk-Luijk CH, Wilson JP. Weight loss and elevated gluconeogenesis from alanine in lung cancer patients. Am J Clin Nutr. 2000;71(2):583-589.

Lou Y-H, Wang J-S, Dong G, Guo P-P, Wei D-D, Xie S-S, et al. The acute hepatotoxicity of tacrine explained by 1 H NMR based metabolomic profiling. Toxicol Res. 2015;4(6):1465-1478.

Pugh CW, Ratcliffe PJ. Regulation of angiogenesis by hypoxia: role of the HIF system. Nature Med. 2003;9(6):677-684.

Braz. J. Pharm. Sci. 2018;54(2):e17604

Page 7 / 8

Roy D, Sheng GY, Herve S, Carvalho E, Mahanty A, Yuan S, Sun L. Interplay between cancer cell cycle and metabolism: Challenges, targets and therapeutic opportunities. Biomed Pharmacother. 2017;89(Suppl C):288-296.

Selak MA, Armour SM, MacKenzie ED, Boulahbel H, Watson DG, Mansfield KD, et al. Succinate links TCA cycle dysfunction to oncogenesis by inhibiting HIF-α prolyl hydroxylase. Cancer Cell. 2005;7(1):77-85.

Semenza GL. HIF-1 and tumor progression: pathophysiology and therapeutics. Trends Molec Med. 2002;8(4):S62-S67.

Tessem MB, Swanson MG, Keshari KR, Albers MJ, Joun D, Tabatabai ZL, et al. Evaluation of lactate and alanine as metabolic biomarkers of prostate cancer using 1H HR-MAS spectroscopy of biopsy tissues. Magnetic Resonance Med. 2008;60(3):510-516.

Willard SS, Koochekpour S. Glutamate signaling in benign and malignant disorders: current status, future perspectives, and therapeutic implications. Int J Biol Sci. 2013;9(7):728.

Yang M, Pollard PJ. Succinate: a new epigenetic hacker. Cancer Cell. 2013;23(6):709-711.

Zu XL, Guppy M. Cancer metabolism: facts, fantasy, and fiction. Biochem Biophys Res Commun. 2004;313(3):459-465.

Page 8 / 8

Braz. J. Pharm. Sci. 2018;54(2):e17604